AUTOMATED REDUCTION OF INSTANTANEOUS FLOW FIELD IMAGES

G. A. Reynolds

M. Short

M. C. Whiffen

Lockheed-Georgia Company

Dept. 72-11, Zone 403

Marietta, Georgia 30063

AUTOMATED REDUCTION OF INSTANTANEOUS FLOW FIELD IMAGES

Abstract. An automated data reduction system for the analysis of interference fringe patterns obtained using the Particle Image Velocimetry technique is described. This system is based on digital image processing techniques which have provided the flexibility and speed needed to obtain more complete automation of the data reduction process. As approached here, this process includes: scanning/searching for data on the photographic record, recognition of fringe patterns of sufficient quality, and finally analysis of these fringes to determine a local measure of the velocity magnitude and direction. The fringe analysis as well as the fringe image recognition are based on full-frame autocorrelation techniques using parallel processing capabilities.

Key words: automated fringe analysis, particle image velocimetry

CONTENTS

1. INTRODUCTION

A number of photographic metrology techniques in solid and fluid mechanics have evolved which rely on multiple exposure recording of particle or speckle images.[1-4] Using these techniques, the translation of a photographed subject is recorded between multiple exposures and used as an instantaneous measure of local in-plane subject motion. For example, in application to fluid flows, an illuminated plane within the flow is the subject and the motion of seeding particles as they follow the flow are recorded from that plane. A typical optical arrangement for such an application is shown in Fig. 1. The resulting photographic recording may then be evaluated to yield an instantaneous velocity field map in the illuminated plane. Due to the quantity and type of data to be evaluated, automation of the data reduction process is instrumental in making these photographic techniques into valuable measurement tools.

Various approaches have been taken for evaluation of the local image displacements from the photographic record. A common approach has been to locally illuminate the film using a small low power laser beam to generate an interference pattern.[5-7] This interference pattern is a parallel set of Young's fringes if the image displacement is uniform within the locality being interrogated. The technique transforms discrete particle or speckle images into a spatial pattern which may be analyzed for its periodic content. Alternately, the local images may be digitized and analyzed directly to obtain their orientation and spacing.[8] The ability to undertake these image processing tasks is enhanced through the use of high speed digital image processing hardware. These capabilities can handle the large quantities of image data involved and provide the flexibility for automation of the various data reduction processes.

The complete automation of the data reduction process consists of a number of stages, including scanning and/or searching of the photograph by the interrogation beam to find data in the form of interference fringes, recognition of good quality fringes, and finally analysis of these fringes to obtain the required information. This process depends on the type of data to be processed, and hence on the manner in which the data was photographically acquired. The data acquisition process is therefore described and can be found in section 2. The subsequent processing of fringe images is discussed in section 3. Finally, the integrated data reduction system is described in section 4 where a reduced set of data is also presented.

2. PHOTOGRAPHIC DATA ACQUISITION

A number of photographic techniques have been utilized to obtain instantaneous velocity field measurements in fluid flows. The Particle Image Velocimetry (PIV) technique has been employed here using a pulsed ruby laser to provide a well collimated light source of sufficient energy density. As was shown in Fig. 1, the laser beam illuminates a thin planar region of the flow field which has been lightly seeded.

This is in contrast to the Laser Speckle Velocimetry (LSV) technique which requires more highly concentrated seeding so that laser speckle is observed instead of actual particle images. The relative merits of the PIV and LSV techniques have been reviewed by Adrian.[9]

The desired application of PIV here is to medium and high speed air flows in wind tunnel studies. The first reported application of this technique in air was due to Meynart[10], who considered a small low Reynolds-number jet. For practical use in most wind tunnel applications a larger probe area is desirable. Therefore a number of difficulties must be addressed in terms of the required laser output energy, the film sensitivity and the provision of adequate flow seeding.

For the application described here a relatively large area was to be probed, covering approximately 130 square centimeters. The probe region was illuminated by a Q-switched ruby laser which was operated in a dual pulse mode. To obtain the required energy density in the illumination sheet the laser was operated in multimode, yielding a total output energy of 2-3 Joules. While this mode of operation provides the needed output energy, a number of problems arise due to the reduced beam collimation in the multimode configuration. These factors are discussed below in particular with regard to selection of an appropriate seeding density.

The illuminated probe plane was imaged from 90 degrees at a magnification close to one using a Schneider 220mm f/5.6 lense. Spherical aberrations, primarily coma, were reduced to an acceptable level by stopping this lense down to between f/8 and f/11. The resulting particle images were recorded on Kodak 2415 cut film which has sufficient resolution (320 lines/mm) and good sensitivity in the red. However due to the required lense settings, it was necessary to preflash the film to a density of 0.3 so that image contrast was optimized.[11] It is apparent that the scattered light levels experienced here were marginal. This is in agreement with the predictions of Adrian[12], which were repeated here for the appropriate seeding material.

As with other laser velocimetry techniques, providing the correct seeding in a wind tunnel application is difficult. This is especially true for PIV where relatively high seeding density must be introduced without affecting the flow quality. In these experiments water droplets generated by an ultrasonic atomizer provided the necessary seeding. While water is less than ideal from an optical standpoint, it was found to be a practical choice for use in the open return wind tunnel facility used here. The resulting particle size was found photographically to be equal to or less than the diffraction limited spot size of the imaging system, that is approximately 20 microns.

In most cases it is desirable to provide a nominal seeding density such that the particles, and hence the resulting data, are continuously distributed. However, using a multimode illumination beam, additional particles are marginally illuminated toward the edges of the sheet. These unwanted particles only contribute to noise in the data reduction

process. This effect was reduced by using relatively sparce seeding so that nominally only one particle image pair would be present in the interrogaton area a time. As a result, the distribution of data on the film could no longer be assumed to be continuous, a fact which the data reduction processes had to accommodate.

Another characteristic of the fringe data which must be recognized by the data reduction system is the presence of cross interference fringes. This is particularly true for dual pulse mode which is most sensitive to the presence of two particle image pairs within the interrogation spot. It is threrefore desirable that the data reduction system be capable of rejecting images having levels of cross interference above some tolerable limit.

3. DATA REDUCTION BY FRINGE ANALYSIS

The question of fringe analysis for the purpose of extracting quantitative information from photographed images is addressed here. With the objective of automation, the approach has been to implement analysis algorithms within the framework of the digital image processing capabilities available. These capabilities include high speed video-rate digitizing, multiple image plane memories, and parallel/pipeline image processing. These processing capabilities allow a series of algebraic and Boolean operations to be performed between image planes in one video frame time. The ability to perform full-frame manipulations is desirable for fringe analysis and is often necessary due to the presence of speckle noise and diffracton halo distortion. Given that parallel analysis of entire fringe images is to be conducted, the speed of the data reduction process is then primarily a function of the relative complexity of a given analysis algorithm.

A general approach to the analysis problem would be the application of a 2-D fast Fourier transform to the fringe image. However this general approach is unnecessarily complex given that a good deal of a priori knowledge is available concerning the fringes being analyzed. That is, the interference pattern should be composed of a parallel array of fringes with the central fringe maximum crossing the center of the diffraction halo. Taking advantage of these properties, a full-frame autocorrelation function similar to that suggested by Meynart[3] has been implemented to extract the fringe spacing in a given direction. This function was obtained by parallel processing the full 512 by 512 fringe image using the relationship:

$$R(d) = \frac{\langle I(-d/2)*I(d/2)\rangle - \langle I\rangle^2}{\langle I^2\rangle - \langle I\rangle^2} \qquad (1)$$

where < > denotes the mean value. In the above expression, the image mean, $\langle I \rangle$, and mean square values, $\langle I^2 \rangle$, are assumed to be constants. This condition is closely approximated by filtering the fringe image with a Gaussian neutral density filter. This filtering process has the added advantage of decreasing the image dynamic range due to the diffraction halo. For each value of the shift, d, a single pass through the video processor is required, corresponding to a single video frame time. The resulting 128 point one-sided autocorrelation function shown in Fig. 2 can be obtained in approximately five seconds. The effectiveness of the full-frame analysis in removing uncorrelated speckle noise is evident in the smoothness of the autocorrelation function. Given this function, a FFT may be performed on the host computer to determine the dominant frequency component.[3] Alternately, since the data is of high quality, a common numerical iteration scheme may be used to find the first peak in R(d). This second method has been used such that only the necessary points of R(d) are calculated in the process. Convergence time along a given analysis direction is typically two seconds.

The above operation must be performed in at least two directions to provide the needed fringe wavelength components from which the velocity magnitude and direction can be determined. However, in general a third direction of analysis is required to resolve the angular ambiguity of plus or minus the resultant fringe angle, as demonstrated in Fig. 3. The actual choice of these three analysis directions should depend on the orientation of the fringes in order to obtain the best resolution.

For an arbitrary fringe orientation, three lines of analysis are chosen from four optional directions: 0, +45, -45, and 90 degrees, such that analysis along a direction closely parallel to the fringes is avoided. The least desirable of the four directions is marked by a dominant frequency component which is significantly lower compared to that found in the other three directions. Again this may be reliably found using the autocorrelation function. To accomplish this quickly, the first minimum in R(d) is found using large steps in "d" as shown in Fig. 4(a). The direction exhibiting the longest approximate wavelength is the least desirable and the analysis may then be continued in the remaining three directions, shown in Fig. 4(b).

The accuracy of the data acquisition and data reduction system is of particular interest. Meynart[3] performed a controlled experiment and found the overall system accuracy to be 1%. It was concluded that the accuracy was ultimately limited by the film resolution, although the individual error contributions were not determined directly. The above conclusion was based on the supposition that the uncertainty in the recorded image position is on the order of the effective film grain size. An effective grain size for a film may be expressed as the inverse of the spatial resolving power, that is 320 lines/mm or 3 microns for Kodak 2415. For particle image sizes on the order of the effective grain size, the uncertainty in the image position may be approximated by this grain size. However assuming a diffraction limit of approximately 20 microns, the image sizes can be expected to be at

least an order of magnitude larger than the effective grain size. Under these circumstances the location of the image centroid, as determined by the interrogating laser beam, is known to a precision significantly better than the effective grain size. These considerations suggest that an accuracy of better than 1% may be possible if other system errors can be kept low. In this respect, the relative merits of the data reduction algorithms need to be addressed.

It is clear that the full-frame autocorrelation function provides significant advantages over less comprehensive analysis techniques. For the subsequent determination of fringe spacing from this autocorrelation function, two techniques have been discussed in this section. The approach taken here has been a direct numerical iteration on the autocorrelation function instead of the more robust but slower FFT of the autocorrelation. The resolution of this numerical iteration is significantly better than one pixel, using curve fitting techniques. This resolution is as good or better than the resolution bandwidth expected from a FFT of the full autocorrelation function. For example if the resolution bandwidth for a FFT calculation is, $B = 1/(m + z)$, where m is the number of correlation values and z is the number of added zeroes[13], then a total record length of 2048 is required to obtain one pixel resolution at a nominal fringe spacing of 50 pixels. This 1-D FFT approach is therefore considered desirable only where significant levels of correlated noise, or cross interference, is present. In such a case it is desirable to select the dominant frequency component.

4. APPLICATION TO REDUCTION OF AERODYNAMIC DATA

The above fringe analysis algorithms have been integrated into an automated data reduction system. This system, shown in Fig. 5, operates on fringe images produced by local coherent illumination of dual particle images recorded on a photograghic film which is indexed by an x-y stage. The flexibility of the digital processing system is exploited here to tailor the reduction process to handle the type of data acquired in this application of the PIV technique.

One of the characteristics of the data considered here is due to the inhomogeneous distribution of seeding particles. While an optimum seeding density is desired, nonuniformities in the flow tend to concentrate these particles in some areas, leaving other areas with relatively sparse seeding. This seeding problem is compounded by the problem of poor illumination sheet definition discussed in section 2. For the above reasons, it is not practical to assume data on a regular grid pattern. The photographic record is therefore scanned using a grid pattern which is modified by a local search if data is not present at a prescribed grid point. This searching scheme is demonstrated in Fig. 6.

A searching scheme such as this assumes that fringe images can be recognized when encountered. This recognition is initially contingent upon an image variance threshold which must be met, thus avoiding areas where no particles are present. Before analysis begins, an image of

sufficiently high variance is further classified to avoid the case of multiple interference patterns. The highly unidirectional character of a good fringe image may be discriminated from a cross-hatched image by considering the four autocorrelation functions used to find the optimum analysis directions, discussed in section 3. As was shown in Fig. 4 the wavelength should vary strongly with angle in a good fringe image. If this is the case, optimum analysis directions can be established. However, if the angular dependence is weak as shown in Fig. 7, the optimum analysis directions cannot be determined with reasonable certainty and the image is rejected because of cross-hatching.

The results produced by the automated data reduction system are described below. The PIV technique has been applied to the flow field about a delta wing at a high angle of attack. For this configuration a pair of vortices are generated by separation of the flow at the sharp leading edge of the wing. The acquisition of instantaneous velocity field measurements is particularly desirable in an unsteady vortex flow field of this type.

This test configuration is shown in Fig. 8. The plan view of half the wing, in Fig. 8(a), shows the axis of the leading edge vortex and the field of view of the probe area. In this measurement the probe plane is close to being co-planar with the wing, diverging from the wing apex by an angle of only 1.5 degrees, as shown in the side view of Fig. 8(b). At this location the probe plane is between the wing surface and the plane of the vortex core. The cross section of the expected vortex flow field is shown in Fig. 8(c). The primary features of the flow include the secondary vortex, V_2, generated by the primary one, V_1, and the secondary separation line, s.i., separating the two.

The automated data reduction system has been used to reduce the photographic data within the area which was shown in Fig. 8(a). This reduced data is shown in Fig. 9. Also shown is the secondary separation line which is evident in the original particle image photograph by the collection of seeding particles along that line. Finally, the approximate location of the primary vortex core projected down to the measurement plane has been drawn at an angle of 11 degrees to the leading edge. The data was obtained at a free stream velocity of 10 m/sec and is typical of the data taken in this turbulent vortex flow using the PIV technique. This particular set of data gives an instantaneous quantitative measure of the unsteady vortex flow and its viscous interaction with the wing surface. These velocity measurements demonstrate the feasibility of this type of instantaneous flow field measurement technique in the wind tunnel application. The increased level of automation has also made the technique more desirable as a research tool.

5. SUMMARY AND CONCLUSIONS

An automated fringe analysis system based on digital image processing techniques has been presented which provides a high level of flexibility

without compromising speed. As a result, a more comprehensive automation of the data reduction process has been made possible. This automated data reduction process includes scanning and searching of the photographic record, recognition of good quality fringes, and analysis of these fringes. The fringe analysis itself is based on a full-frame autocorrelation which collapses the the available information into a function of a single variable, minimizing uncorrelated noise in the process. Since noise has been minimized without loss of coherent information, the autocorrelation provides an accurate basis from which the wavelength component in a given direction may be computed.

The actual technique used to obtain the wavelength from the autocorrelation function may be varied depending on the level of noise and cross interference present in the image. For nominal noise levels and low levels of cross interference a numerical iteration to find the wavelength has been advantageous. The accuracy of these measurements should not be limited to 1% by the available film resolution. However, for high levels of cross interference an FFT of the autocorrelation function may be necessary to isolate the desired frequency component.

Simplification of the data reduction process should result from improvements in the quality of the photographic data. Significant improvements may be be attained through use of a monomode laser and improved seeding material. Problems with cross interference will be reduced by multiple pulsing instead of just dual pulse illumination. This will also improve accuracy through the effective thinning of the fringes. Further reductions of cross interference problems may be obtained by adjusting the interrogation spot diameter based on the local flow scales.

6. REFERENCES

1. E. Archbold and A. E. Ennos, Opt. Acta 19, 253 (1972).

2. P. G. Simpkins and T. D. Dudderar, J. Fluid Mech. 89(4) (1978).

3. R. Meynart, Applied Optics 22(4), 535 (1983).

4. L. M. M. Lorenco and M. C. Whiffen, in Proceedings, Second International Symposium on Application of Laser Anemometry to Fluid Mechanics, 6.3 (1984).

5. G. H. Kaufmann, A. E. Ennos, B. Gale, and D. J. Pugh, J. Phys. E: Sci. Instrum. 13, 579 (1980).

6. R. Meynart, Rev. Sci. Instrum. 53(1), 110 (1982).

7. D. W. Robinson, Applied Optics 22(14), 2169 (1983).

8. C. S. Yao and R. J. Adrian, Applied Optics 23(11), 1687 (1984).

9. R. J. Adrian, Applied Optics 23(11) 1690 (1984).

10. R. Meynart, Phys. Fluids 26(8), 2074 (1983).

11. M. J. Eccles, M. E. Sim, and K. P. Tritton, Low Light Level Detectors in Astronomy, Chap 3, Cambridge University Press, New York (1983).

12. R. J. Adrian and C. S. Yao, in Proceedings, Second International Symposium on Application of Laser Anemometry to Fluid Mechanics, 6.4 (1984).

13. J. S. Bendat and A. G. Piersol, Random Data: Analysis and Measurement Procedures, Chap. 9, Wiley-Interscience, New York (1971).

List Of Figure Captions

Fig. 1 Optical configuration for Particle Image Velocimetry.

Fig. 2(a) Full-frame one-sided autocorrelation function in the horizontal direction.

Fig. 2(b) Digitized fringe image (512 x 512), corresponding to Fig. 2(a).

Fig. 3 Fringe angle sign ambiguity for analysis in only two directions.

Fig. 4 Determination of optimum analysis directions, (a) Autocorrelation along the four optional directions, (b) Corresponding fringes and optimum analysis directions.

Fig. 5 Automated data reduction system, F-film plane, L-lense, S-beam stop and Gaussian neutral density filter.

Fig. 6 Scanning/searching routine, *-successful data analysis

Fig. 7 Fringe image recognition, (a) Autocorrelation of image with low angular dependence, (b) Fringe image rejected because of cross-interference.

Fig. 8. Aerodynamic test configuration, (a) Plan View; L.E.-leading edge, Σ-measurement area, σ-reduced data, s.l.-secondary separation line, V_1-primary vortex core, (b) Side View; W-wing surface, (c) Cross section C; S-secondary separation point, V_2-secondary vortex.

Fig. 9. Reduced data, L.E.-leading edge, s.l.-secondary separation line, V_1-primary vortex core.

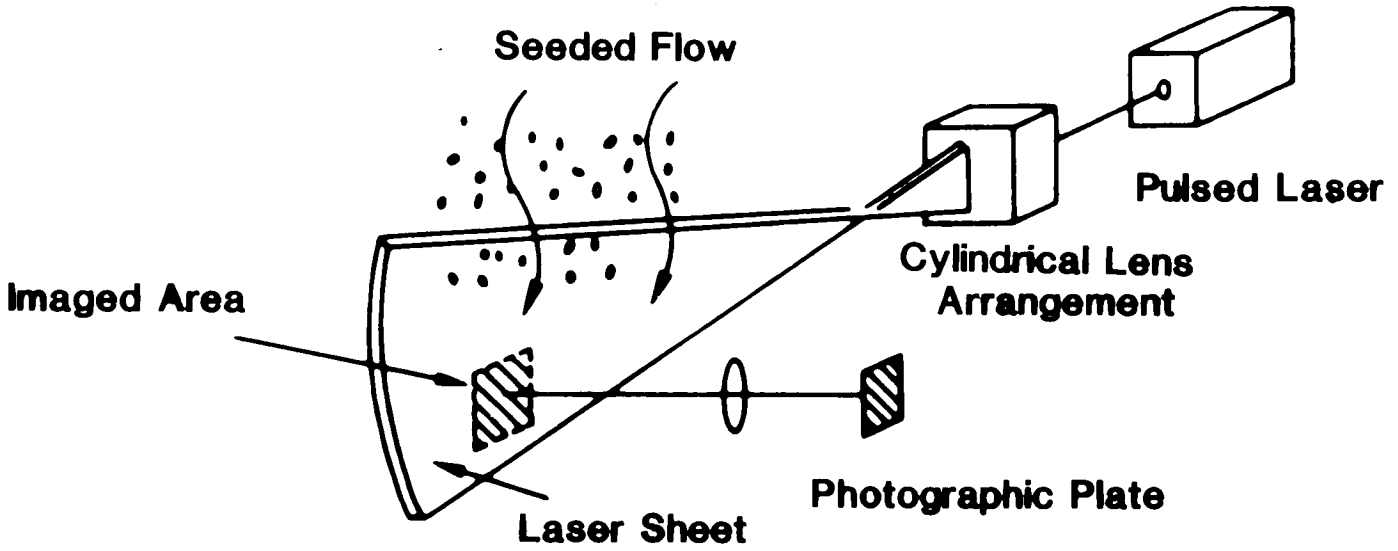
Seeded Flow
Pulsed Laser
Cylindrical Lens
Arrangement
Imaged Area
Photographic Plate
Laser Sheet

Fig. 1

a

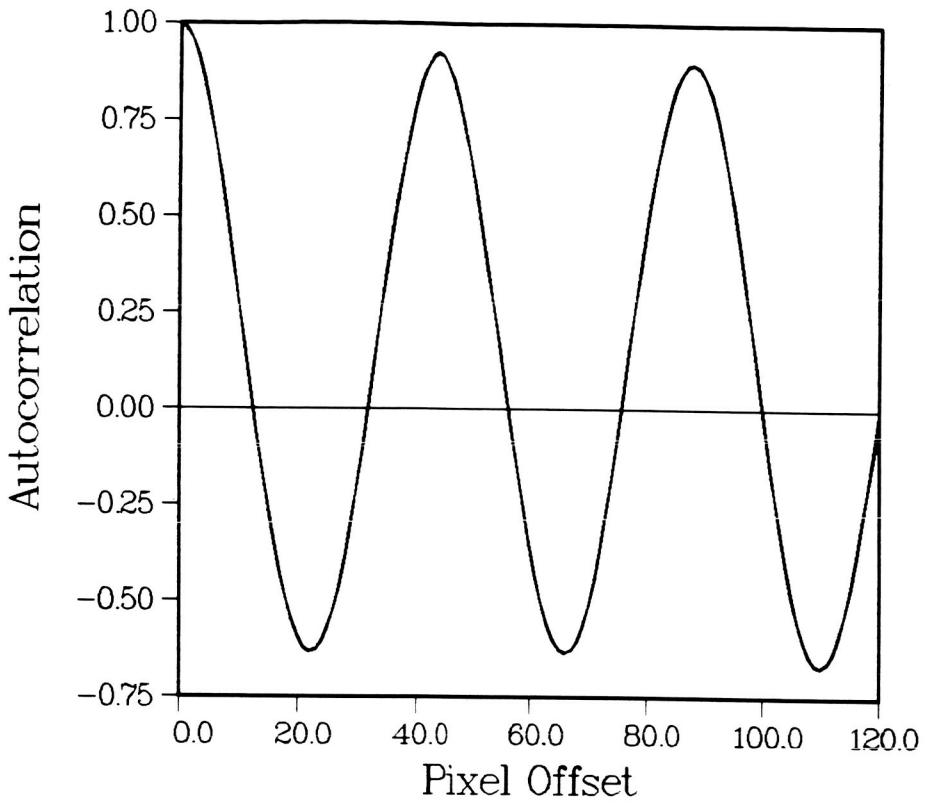
1.00
0.75
0.50
0.25
0.00
-0.25
-0.50
-0.75
Autocorrelation
0.0
20.0
40.0
60.0
80.0
100.0
120.0
Pixel Offset

b

Fig. 2

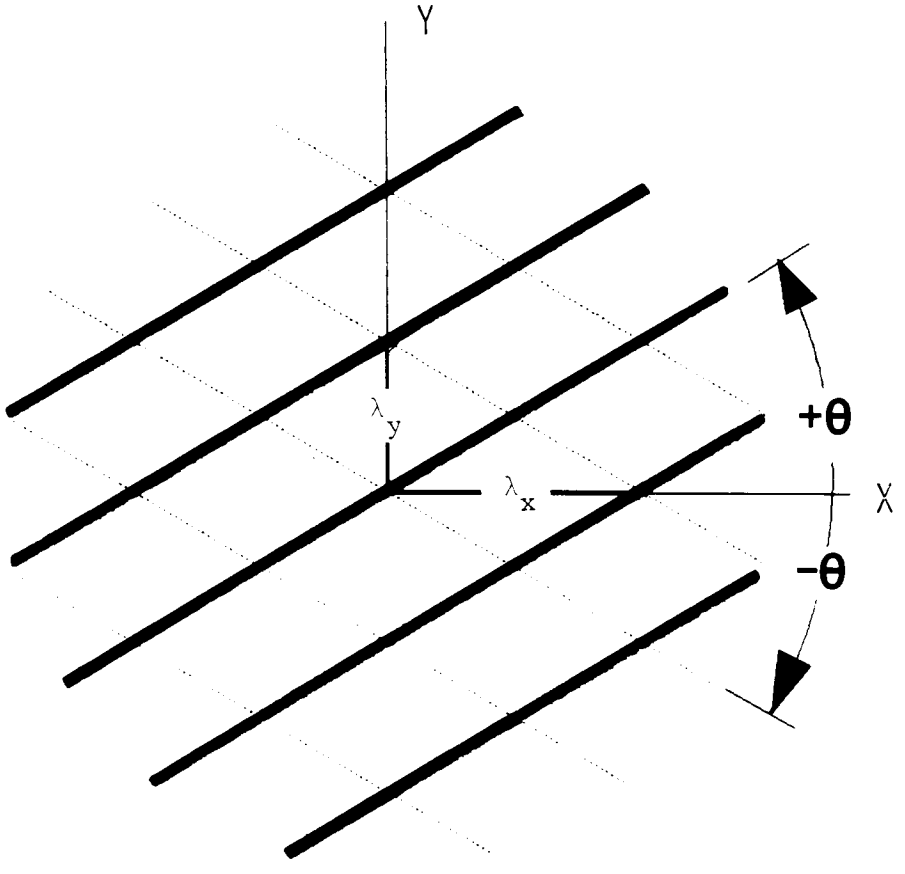

Fig. 3

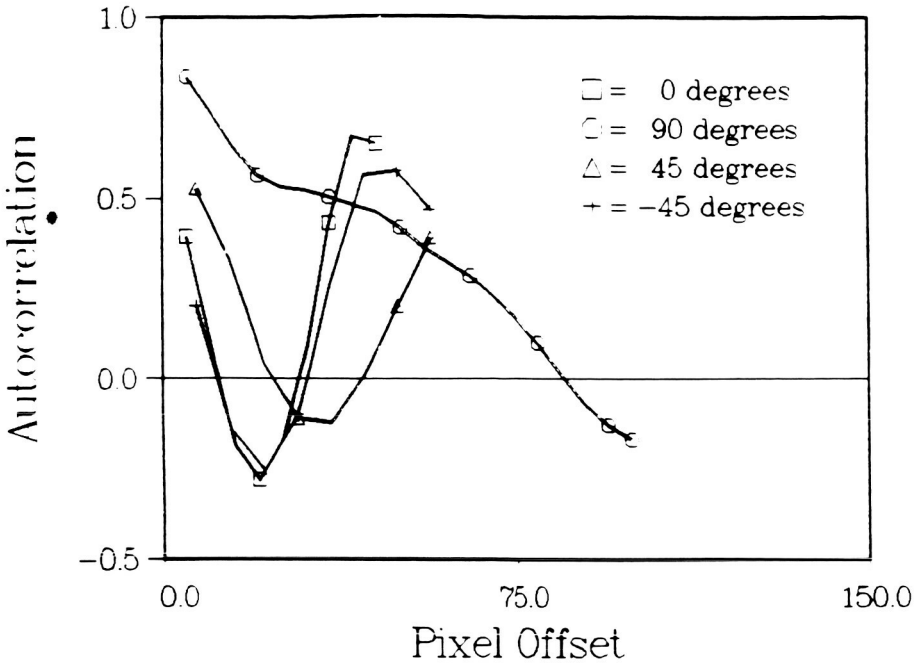
1.0
0.5
0.0
-0.5
Autocorrelation
□ = 0 degrees
○ = 90 degrees
△ = 45 degrees
+ = −45 degrees
0.0
75.0
150.0
Pixel Offset

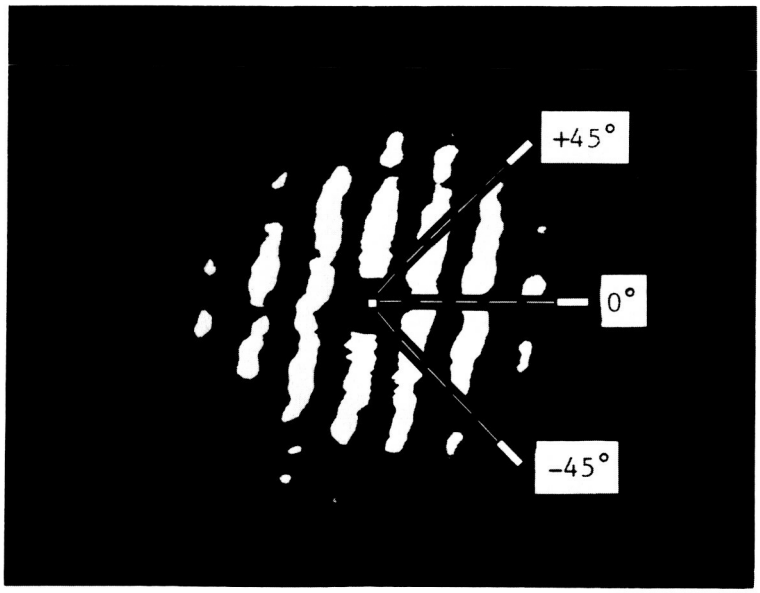
+45°
0°
-45°

Fig. 4

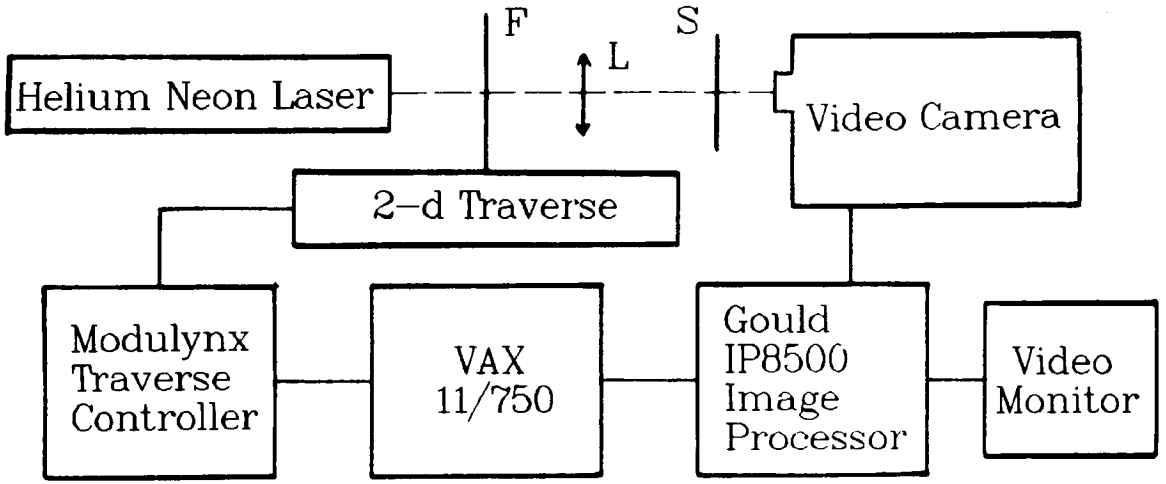
F
S
L
Helium Neon Laser
Video Camera
2–d Traverse
Modulynx
Traverse
Controller
VAX
11/750
Gould
IP8500
Image
Processor
Video
Monitor

Fig. 5

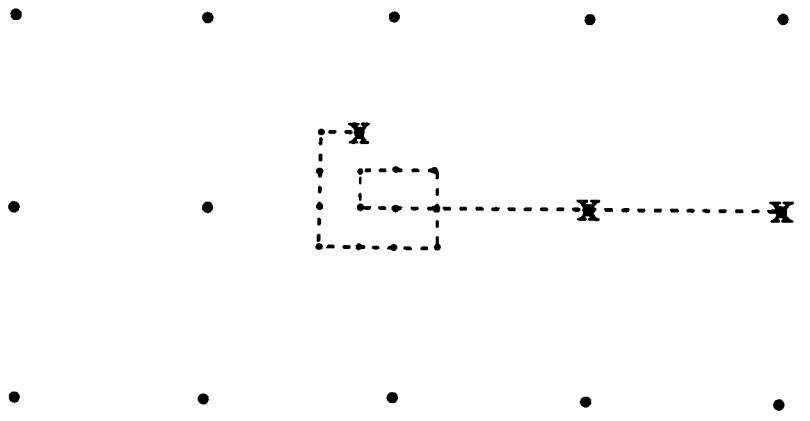

Fig. 6

a

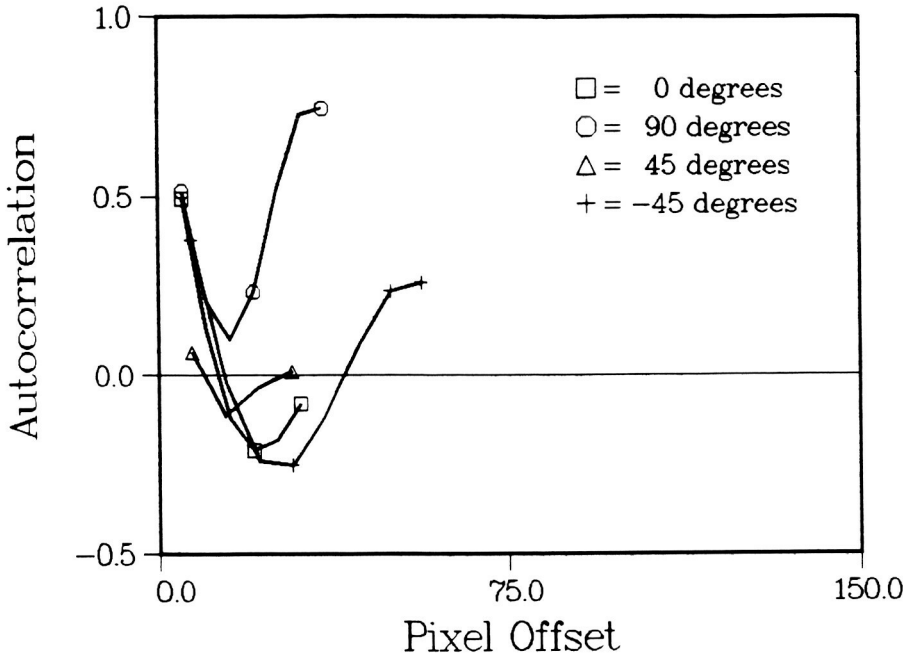
1.0
0.5
0.0
−0.5
Autocorrelation
□ = 0 degrees
○ = 90 degrees
△ = 45 degrees
+ = −45 degrees
0.0
75.0
150.0
Pixel Offset

b

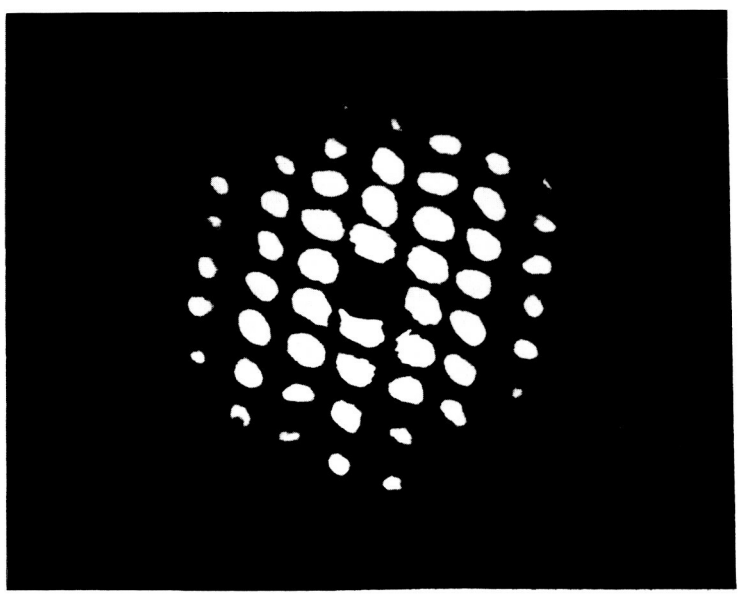

Fig. 7

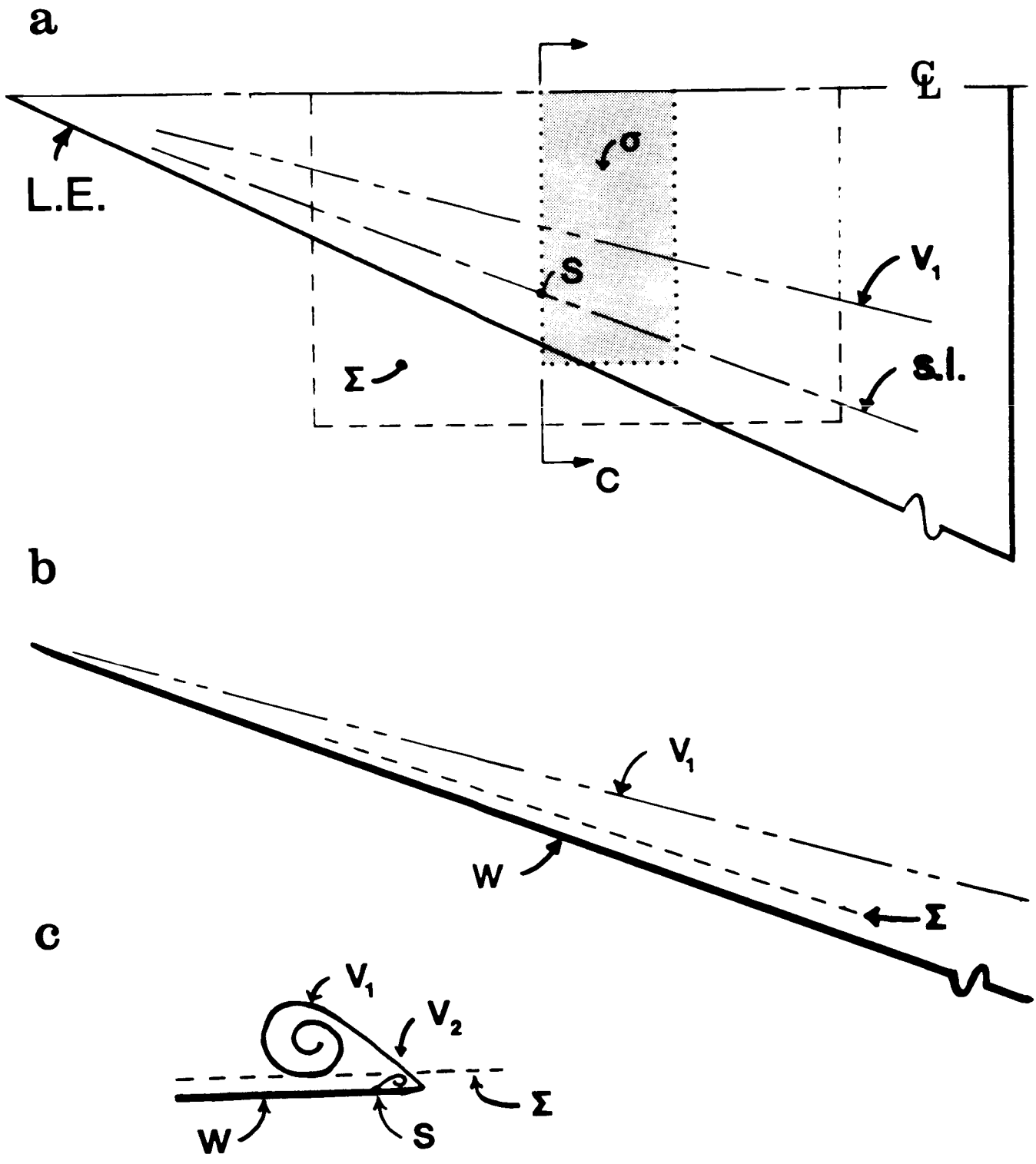

Fig. 8

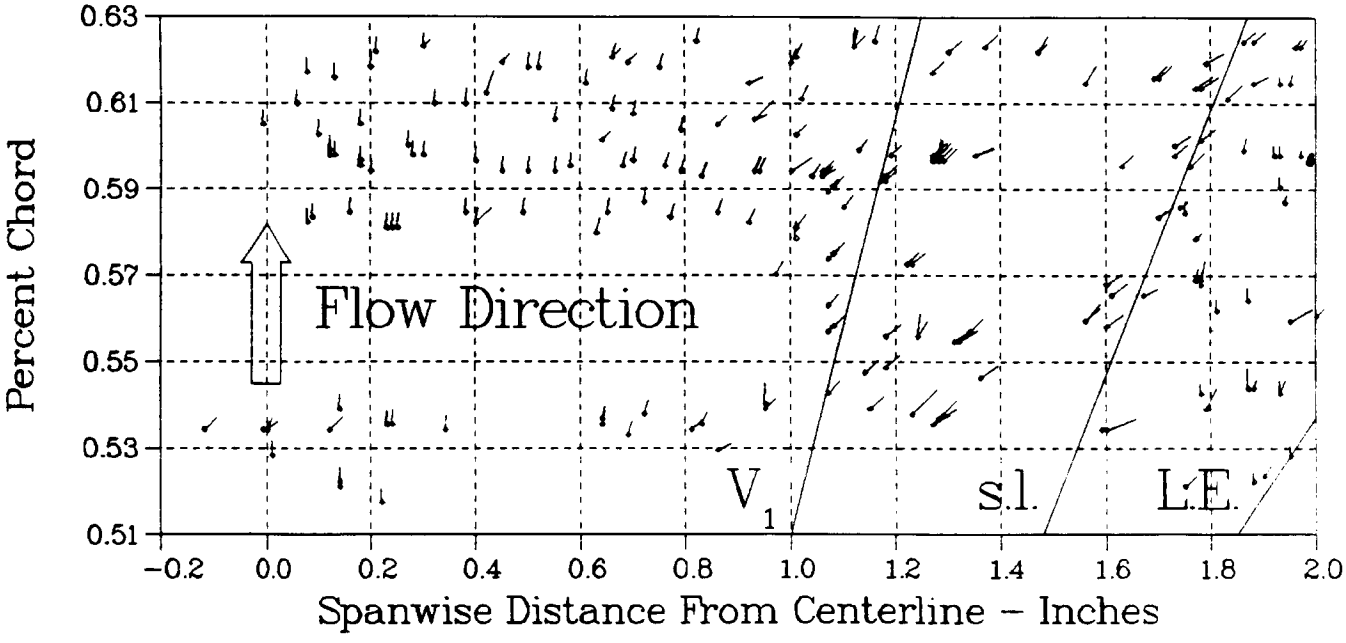
0.63
0.61
0.59
0.57
0.55
0.53
0.51
Percent Chord
Flow Direction
V1
s.l.
L.E.
-0.2
0.0
0.2
0.4
0.6
0.8
1.0
1.2
1.4
1.6
1.8
2.0
Spanwise Distance From Centerline - Inches

Fig. 9